Journal of Materials Chemistry C

Large Piezoelectric Response of van der Waals Layered Solids

Journal:	*Journal of Materials Chemistry C*
Manuscript ID	TC-ART-05-2018-002560.R1
Article Type:	Paper
Date Submitted by the Author:	14-Aug-2018
Complete List of Authors:	Manna, Sukriti; Colorado School of Mines, Mechanical Engineering Gorai, Prashun; Colorado School of Mines, Physics; National Renewable Energy Laboratory, Brennecka, Geoff; Colorado School of Mines, Metallurgical and Materials Engineering Ciobanu, Cristian; Colorado School of Mines, Division of Engineering Stevanovic, Vladan; Colorado School of Mines, Physics

SCHOLARONE™
Manuscripts

Journal Name

ARTICLE TYPE

Cite this: DOI: 10.1039/xxxxxxxxxx

Large Piezoelectric Response of van der Waals Layered Solids†

Sukriti Manna,[a,b], Prashun Gorai,[a,b], Geoff L. Brennecka,[a] Cristian V. Ciobanu,[a] and Vladan Stevanović*[a,b]

Received Date
Accepted Date

DOI: 10.1039/xxxxxxxxxx

www.rsc.org/journalname

The bulk piezoelectric response, as measured by the piezoelectric modulus tensor (**d**), is determined by a combination of charge redistribution due to strain and the amount of strain produced by the application of stress (stiffness). Motivated by the notion that less stiff materials could exhibit large piezoelectric responses, herein we investigate the piezoelectric modulus of van der Waals (vdW) layered materials using first-principles calculations. From a pool of 869 known binary and ternary quasi-2D layered materials, we have identified 135 non-centrosymmetric crystals of which 51 are found to have piezoelectric modulus tensor (**d**) components larger than the longitudinal piezoelectric modulus of AlN, a common piezoelectric for resonators. We have also identified three materials with **d** components larger than that of $PbTiO_3$, which is among the materials with largest known piezoelectric modulus. None of the identified materials have previously been considered for piezoelectric applications. Furthermore, we find that large **d** components are always coupled to the shear or axial deformations of the vdW gap between the layers and are indeed enabled by the weak inter-layer interactions.

1 Introduction

Coupling between the mechanical degrees of freedom and the electric polarization in a solid, a hallmark of piezoelectric materials, has found use in applications that range from sensors, resonators, motors, and actuators, to high-resolution ultrasound devices and miniature filters for cellular communications.[1–3] Interestingly, only about 10 piezoelectric materials, including SiO_2 (quartz), $LiTaO_3$, $LiNbO_3$, PZT (lead zirconate titanate)-based, $BaTiO_3$-based, $(K,Na)NbO_3$-based, $Bi_4Ti_3O_{12}$-based, AlN, and ZnO, are technologically relevant and cover virtually all of these applications.[4–6] Expanding the pool of known piezoelectric materials would help broaden the range of applications and allow earth-abundant and non-toxic[7] replacements for materials that are presently in use. Furthermore, it would offer more cost- and performance-effective choices beyond a relatively limited set of materials that are at present used for piezoelectrics. The need for new piezoelectrics was recognized before and was the main motivation behind recent computational efforts in high-throughput screening of inorganic materials for piezoelectric performance. These include the work on perovskite alloys,[8,9] and creation of a database of piezoelectric properties of compounds.[10] Materials with reduced dimensionality, such as 2D mono- and multi-layers have also been investigated recently.[11–17] Centrosymmetric layered materials such as MoS_2 and BN, which are not piezoelectric in their bulk form, exhibit piezoelectric response when reduced to single atomic layers, which themselves are not centrosymmetric.[16] In the mono-layer limit piezoelectricity can also be engineered by surface modification by appropriately chosen adsorbate species.[18–20]

In virtually all of these works, the quantity of interest was the

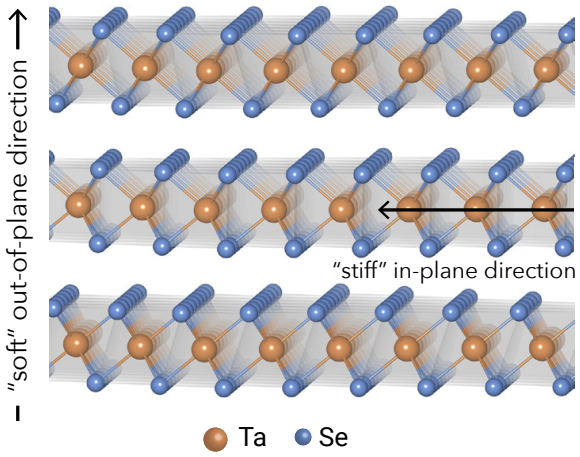

Fig. 1 Illustration of a quasi-2D material ($TaSe_2$), showing the atomic structure of the layers and the van der Waals spacing between them.

[a]Colorado School of Mines, Golden, CO 80401. [b]National Renewable Energy Laboratory, Golden, CO 80401. E-mail: vstevano@mines.edu

† Electronic Supplementary Information (ESI) available

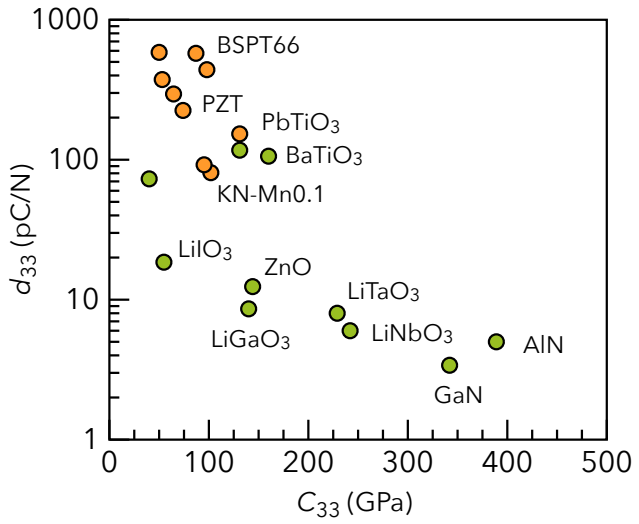

Fig. 2 Correlation between experimentally-measured longitudinal piezoelectric modulus (d_{33}) and their elastic modulus (C_{33}). Green circles denote data from either single crystals or single-crystal single-domain samples in case of ferroelectric materials. Orange circles denote polycrystalline samples. Data is sourced from Refs. 1,2,24–29.

piezoelectric coefficient tensor e_{ij}, which relates the polarization P_i to strain ε_j,[21,22] (in Voigt notation,[23] $P_i = \sum_j e_{ij}\varepsilon_j$) and is typically obtained from first-principles calculations. Here, we also apply first-principles calculations to screen for candidate piezoelectric materials, but instead of the piezoelectric coefficient tensor we consider the piezoelectric modulus tensor d_{ij}, which relates the induced polarization to the applied stress, $P_i = \sum_j d_{ij}\sigma_j$.[21,22] The advantage of using d_{ij} is in that it represents an important figure of merit in a wide range of technological applications[1,2] and is a more commonly measured piezoelectric property, especially for materials in the thin film form. Because the induced polarization depends on the applied stress through a combination of the charge redistribution due to strain and the amount of strain that is produced by the applied stress, the piezoelectric modulus tensor d_{ij} depends on both the piezoelectric coefficient tensor e_{ij} and the elastic tensor C_{ij} as:

$$d_{ij} = \sum_{k=1}^{6} e_{ik}(C^{-1})_{kj}. \quad (1)$$

From equation (1), we can infer that large piezoelectric modulus d_{ij} can be expected in materials with large e_{ij}, but also in systems with low stiffness C_{ij}. Softer (less stiff) materials can exhibit large piezoelectric response, as measured by d_{ij}, compared to stiffer materials with similar e_{ij}. This is illustrated in Figure 2, where we notice less stiff materials overall exhibit larger piezoelectric moduli in the corresponding direction.

For this reason, we concentrate our investigation on van der Waals (vdw) layered (quasi-2D) materials, which can be expected to have relatively low stiffness in the out-of-plane direction due to the presence of weak vdW interactions between the layers. The questions we are addressing are: (a) whether materials that belong to this class and exhibit large piezoelectric modulus (d_{ij}) can be found, and (b) if this is true, what is the role of the vdW interactions in enabling the strong response. To our knowledge, these questions have not been previously addressed in a systematic way.

Our results confirm the expectations. The search has revealed a number of vdW layered materials with relatively large d_{ij} components. Out of 869 considered binary and ternary vdW layered structures, we have identified 135 non-centrosymmetric crystals. Out of those, we found more than one third of the structures (51) that exhibit piezoelectric moduli larger than that of AlN (d_{33}=5.5 pC/N), a commonly used piezoelectric material in resonator applications. In addition, we found three structures with piezoelectric moduli even larger than that of $PbTiO_3$ (d_{33}=119 pC/N), another established piezoelectric material known for its very large response. It is important to note that none of these identified vdW materials have previously been considered for piezoelectric applications.

From an in-depth analysis of the coupling between stress (σ) and piezoelectric modulus (**d**) components, we find that in all of these materials, large piezoelectric moduli are always coupled to the stress components that induce axial or shear deformations of the van der Waals gaps between the layers. This is consistent with the fact that smaller elastic constants are related to these deformations. Overall, our results highlight the vdW layered materials as a rich chemical and structural space for discovering new piezoelectric materials, and introduce the role of elastic properties as an additional design criteria for finding materials with large piezoelectric modulus.

2 Computational Methodology

The details of the computational methodology used in this work are discussed in this section, which is broadly divided into three subsections. The first subsection describes the procedure for identifying vdW layered structures from the Inorganic Crystal Structure Database (ICSD).[30,31] Next, we describe the drawbacks of the GGA exchange-correlation functionals in predicting the properties of vdW layered materials and our approach to overcome this issue. In the final subsection, we provide a detailed workflow for evaluating the piezoelectric modulus tensor (**d**) of quasi-2D materials.

2.1 Automated Identification of Quasi-2D Materials

An essential aspect of this work is the identification of vdW layered (quasi-2D) materials from the ICSD. To accomplish this, we extend our previously-developed procedure[32] for automated identification of binary quasi-2D materials to include ternary chemistries. Similar algorithms have been developed by others for the purpose of identifying vdW layered structures, including the work by Ashton *et al.*,[33] Mounet *et al.*,[34] and Cheon *et al.*[35]

Our procedure relies on a slab cutting routine and bond counting. As a first step, stoichiometric slabs of a certain thickness for all symmetry-inequivalent sets of Miller indices (hkl) within a certain range ($-3 \leq h,k,l \leq 3$) are created. Next, for each slab, the surface termination that minimizes the number of broken bonds is determined by translating surface atoms from one side of the slab to the other using appropriate lattice vectors. For the determined

This journal is © The Royal Society of Chemistry [year]

surface termination, the minimal number of broken bonds, *i.e.*, under-coordination, of the surface atoms is counted. Therefore, a crystal structure is considered quasi low-dimensional when there exists at least one (hkl) direction for which the corresponding slab does not have any under-coordinated surface atoms relative to the bulk coordination in the first shell. If there is exactly one (hkl) direction that satisfies this condition, the structure is a layered (quasi-2d) material. If more than one (hkl) directions satisfy this condition, then the crystal structure is of lower dimensionality; if exactly two such (hkl) directions exists, it is a quasi-1D structure and a molecular crystal, if more than two (hkl) satisfy the condition. When no such directions exists, the material is considered a three-dimensional structure.

In Ref. 32, we demonstrated the success of this approach in searching quasi-2D materials, including complex materials with layer stacking in oblique directions, corrugated layers, and layers composed of multiple atomic layers. In this work, we have considered ∼3500 binary and ∼8000 ternary compounds from the ICSD to search for vdW layered (quasi-2D) materials. We restricted our search to stoichiometric and ordered systems that do not contain rare earth elements and less than 50 atoms in the unit cell. From this search, we have identified 426 binary and 443 ternary quasi-2D materials. The complete list of the identified quasi-2D materials is provided in the supplementary information.

2.2 Calculation of Piezoelectric Properties

In quasi-2D materials, the individual layers are held together by relatively weak vdW interactions. The standard exchange-correlation functionals typically employed in density functional theory (DFT) calculations, including the calculations of elastic and piezoelectric properties, are known to perform poorly in describing the vdW interactions. This is evident from the relatively large errors in the out-of-plane lattice constants and the associated elastic properties.[36] To overcome this issue, we employed a vdW-corrected functional (optB86) as implemented in the Vienna Ab-initio Simulation Package (VASP) code[37,38] to calculate the lattice parameters, elastic, and piezoelectric properties of quasi-2D materials.[39,40] To evaluate the piezoelectric coefficient tensors, we utilize the VASP implementation of the density functional perturbation theory (DFPT)[41–43] calculations. A relatively large plane wave cutoff energy of 540 eV is used for structural relaxation, calculation of elastic tensors and piezoelectric coefficient tensors. A dense k-point grid, defined by $n_{\text{atoms}} \times n_{\text{kpoints}} \approx 1000$, where n_{atoms} is number of atoms in the primitive cell and n_{kpoints} is the number of k-points, is employed. In all our calculations, a very high tolerance of 10^{-8} eV for energy convergence is used, which is an important consideration for conducting DFPT calculations.[10] For calculation of elastic tensors, we use a finite difference method. Here, the full elastic tensor is calculated by conducting six finite distortions of the lattice and obtaining elastic constants (C_{ij}) from the stress-strain relationship.[44–47]

The importance of incorporating vdW interactions is illustrated in Figure 3, where we notice a significant improvement in predicting elastic constants, particularly C_{33} and C_{44}, with the vdW-corrected functional (optB86)[39,40] compared to the standard

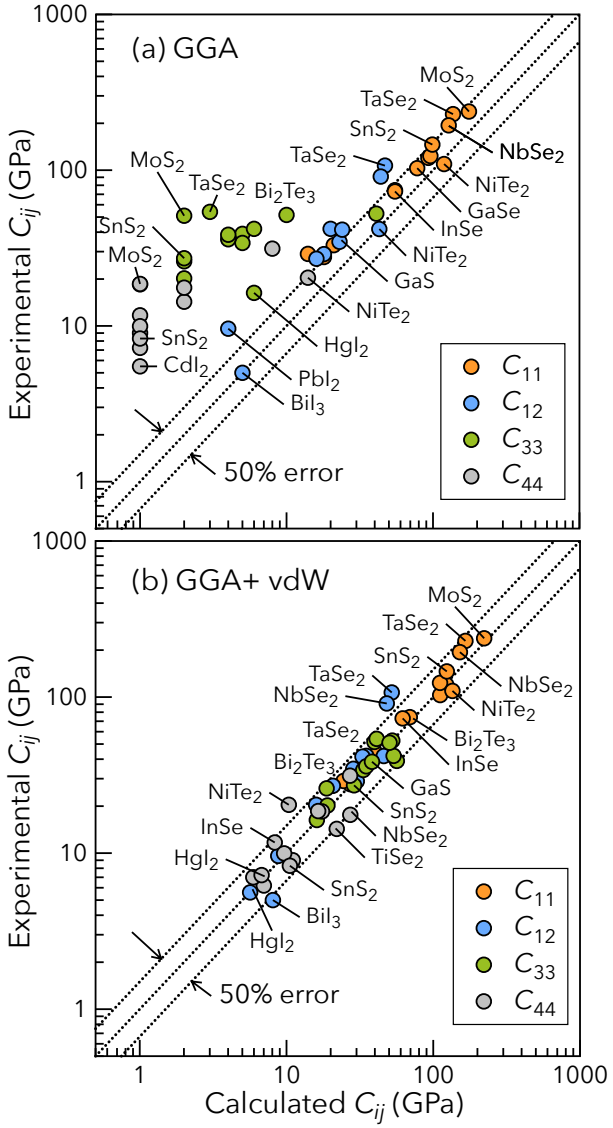

Fig. 3 Elastic constants of quasi-2D materials calculated with (a) GGA and (b) vdW-corrected functional. The calculated values are compared with experimentally-measured values. The calculations with the vdW-corrected functional are all within 50% error relative to the measurements. Details of measurement techniques, measurement temperatures, *etc.*, are provided in the supplementary information.

GGA-PBE functional.[48] The GGA-PBE predicted elastic constants are sourced from Ref. 49. A more detailed analysis of the data presented in Figure 3 reveals that the GGA-PBE is still better in predicting in-plane elastic coefficients C_{11} and C_{12}, but the error in reproducing C_{33} and C_{44} is a factor of 10 or larger. This is due to the fact that C_{33} and C_{44} are directly related to the deformations of the vdW gaps between the layers and the failure of GGA-PBE in describing weak vdW interactions.The calculations of elastic constants are all within 50% error relative to the measurements. The comparison of predicted properties with GGA-PBE and vdW-corrected functional is limited only to the elastic constants(Figure 3 b); the lack of experimental data on piezoelectric properties of layered materials prevented us from making similar comparisons for predicted piezoelectric properties. In Table S1

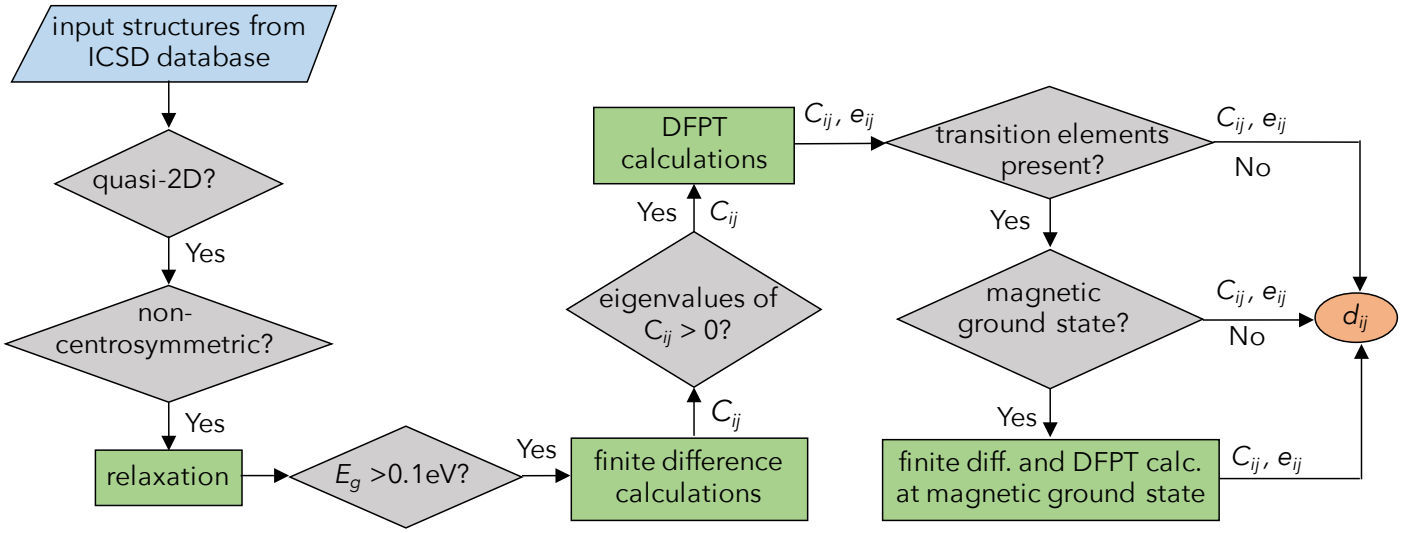

Fig. 4 Workflow for calculations of piezoelectric coefficient tensor e_{ij}, the elastic stiffness C_{ij}, and the piezoelectric modulus tensor d_{ij} of quasi-2D materials. A vdW-corrected functional is used in all calculations.

in the supplementary information, we provide the experimental details (*e.g.* measurement techniques, measuring temperatures, *etc.*) for each compound shown in Figure 3. The comparison of calculated and experimental values of the piezoelectric modulus of few commercially-important piezoelectric materials, including AlN and $PbTiO_3$, are provided in the supplementary information (Figure S1). The calculated piezoelectric moduli d_{33} are within 20% error relative to the measured values.

2.3 Workflow for Identification of Quasi-2D Piezoelectrics

A complete workflow we developed for identifying promising quasi-2D piezoelectric materials is illustrated in Figure 4. The binary and ternary crystal structures from the ICSD database are first screened using the automated algorithm for identifying quasi-2D structures. Then, we filter out all centrosymmetric structures based on the space group assigned in ICSD. Out of ∼11500 binary and ternary materials we find 869 layered systems, out of which 135 are identified as having non-centrosymmetric structures. It is to be noted that the piezoelectricity can be engineered by introducing defects and doping in centrosymmetric structures as well.[18,50] Such artificially formed piezoelectricity can be important as an alternative way for designing new piezoelectric materials.

Next, the non-centrosymmetric, structures are relaxed using the previously described first-principles calculations employing a vdW-corrected functional. As the piezoelectric materials need to have sizable band gaps for their properties to not be screened by the existence of free charge carriers we next employ a band-gap filter. As suggested in the previous works,[32,51] for electronic structure calculation, we perform self-consistent GGA-PBE calculations on the vdW-relaxed structures using dense k-point grids. Because of the known band gap error in DFT calculations we use a band gap cutoff of 0.1 eV. Fifty additional materials with their band gap smaller than 0.1 eV are discarded as a result. Finite difference calculations are performed with vdW-corrected functional to obtain the elastic constants (**C**). Five materials with elastic tensors with negative eigenvalues are also discarded. According to Born stability criteria,[52] the elastically stable materials always have positive eigenvalues of stiffness matrix. This means that an elastically stable materials always have positive elastic energy for arbitrary homogeneous deformation by an infinitesimal strain.[53] With the remaining 80 candidates, we proceed our calculations by performing Density Functional Perturbation Theory (DFPT)[41–43] calculations to assess their piezoelectric coefficient tensor, **e**. Out of the remaining 80 candidates, 38 materials contain transition metal elements. For these, we perform a limited search of the magnetic ground state by enumerating all magnetic configurations in the unit cell and calculating their total energies. The elastic and piezo calculations are then performed only on the lowest energy spin state. This step is necessary because of the strong dependence of the electronic structure and other properties on spin configuration discussed in more details in Ref. 54. The automated DFT calculations including initial file generation, calculating properties, data extraction, and data handling are performed with the help of PyLada,[55] a Python framework for high-throughput first-principles calculations. In summary, vdW-corrected functional is used for structural relaxations and calculations of elastic (**C**) and piezoelectric coefficient (**e**) tensors. The electronic structures are calculated with GGA-PBE functional on the relaxed structures.

3 Results and Discussions

3.1 Promising Quasi-2D Piezoelectric Materials

Based on the calculated piezoelectric modulus tensor, a number of candidate materials with relatively large d_{ij} components have emerged. They are shown in Figure 5 with the full list together with the corresponding d_{ij}, C_{ij}, and e_{ij} values provided in the supplementary information. In addition, the top 20 most promising systems, based on the largest d_{ij} component, are listed in Table 1.

The piezoelectric modulus tensor (**d**) is a third rank tensor, and

This journal is © The Royal Society of Chemistry [year]

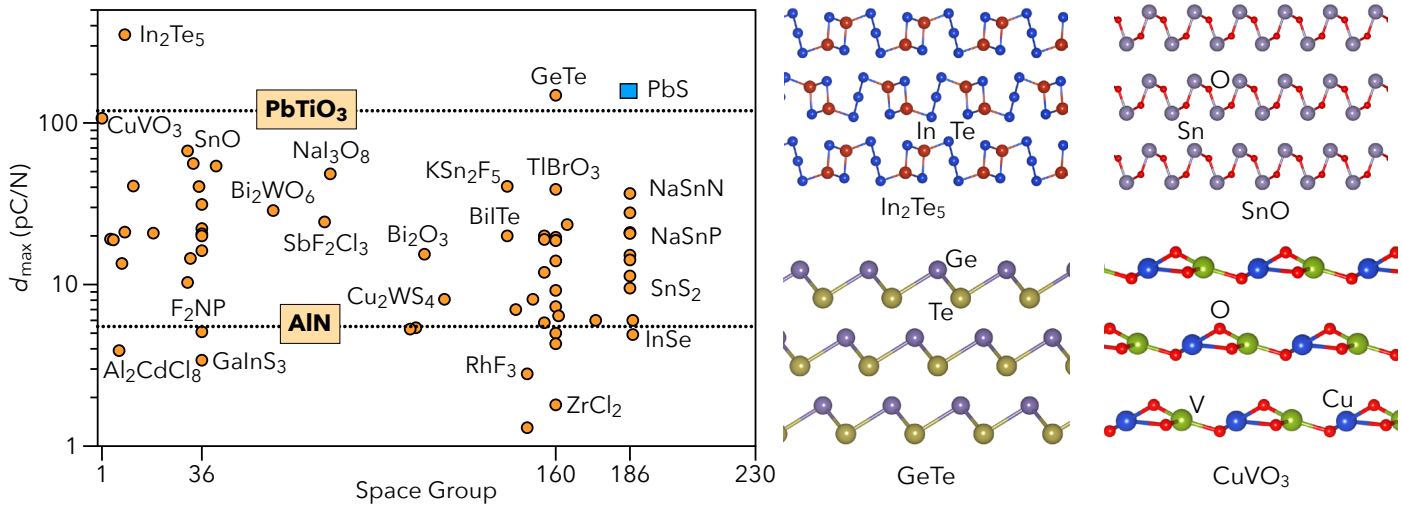

Fig. 5 Left: Plot of $d_{max} = max(|d_{ij}|)$ as a function of the space group number for 63 vdW layered materials (out of 135 non-centrosymmetric structures) with finite piezoelectric response. The two horizontal dotted lines denote the d_{33} values of $PbTiO_3$ (119 pC/N) and AlN (5.5 pC/N). The blue square in this plot represents the hypothetical structure of PbS (distorted NiAs found in ICSD), which is not the ground-state rocksalt structure. Right: crystal structures of vdW layered materials with predicted large piezoelectric moduli.

any isotropic averaging scheme will yield zero.[56] To rank these materials based on the merit of their piezoelectric response, we define $d_{max} = max(|d_{ij}|)$ as the largest element of the absolute d_{ij} matrix. Then the d_{max} is plotted against the space group number in Figure 5. Additionally, we have calculated the magnitude of d_{max} of several candidate materials using Grimme D3[57] and self-consistent Tkatchenko & Scheffler (SCTS)[58] vdW-corrected functionals. For these candidate materials, the predicted d_{max} values are even larger with D3 and SCTS functionals compared to optB86. A comparison of d_{max} calculated with optB86, D3, and SCTS functionals can be found in Table S2 in the supplementary information. The two reference lines in Figure 5 have been drawn for categorizing these candidates – one representing calculated d_{33} of $PbTiO_3$ and the other representing calculated d_{33} of AlN (see supplementary information for the benchmark against experiments). Note that $PbTiO_3$ is also a ferroelectric material and here we are only using the value for its piezoelectric response. More precisely, the $PbTiO_3$ reference line corresponds to the bulk piezoelectric modulus corresponding to the single-crystal single-domain samples.

The materials shown in the left panel of Figure 5 can broadly be divided in three categories. The first category is comprised of quasi-2D compounds with d_{max} larger than the longitudinal piezoelectric modulus of $PbTiO_3$ (d_{33}=119 pC/N)[1] – the key end member of most commercial high-strain piezoelectrics. We found three materials (In_2Te_5, PbS, and GeTe) in this category. Among them PbS is not in its ground state rocksalt phase, but in the hypothetical distorted NiAs structure which has found its way into the ICSD.[59] The other two compounds have previously been experimentally synthesized,[60,61] but their piezoelectric moduli have not been reported so far.

In the second category, we group all compounds which have d_{max} larger than the longitudinal piezoelectric modulus of AlN (d_{33}=5.5 pC/N)[62] and lower than the longitudinal piezoelectric modulus of $PbTiO_3$. The majority (48 compounds) of the piezoelectric candidates from our study fall in this category revealing that overall the vdW bonded quasi-2D systems indeed exhibit a propensity toward large piezo-response. This group is composed from oxides and other chalcogenides such as $CuVO_3$, SnO, $BiInO_3$, MoV_2O_8, SnS_2, InSe, Cs_2Te_3 and other (total of 30); halides such as KSn_2F_5, AgI, $MgCl_2$, and PbI_2 (total of 4); pnictides such as NaSnN, NaSnP, KSnAs, and NaN_3 (total of 4). Also, a number of materials in this group (10 compounds) are the mixed anion systems, *e.g.,* NaI_3O_8, SbF_2Cl_3. Not surprisingly, the more ionic systems like oxides, halides, and nitrides are more frequently found closer to the top of the range. Finally, two compounds Cs_2Te_3 and Bi_2WO_6 are found in calculations to be dynamically unstable, but both have been experimentally synthesized (likely high-temperature phases).[63,64]

The last group is composed of materials with the piezoelectric response lower than the longitudinal piezoelectric modulus of AlN. Though these candidates exhibit low piezoelectric responses, they could still be useful as the calculated moduli are comparable with that of quartz (d_{11}=2.27 pC/N).[65] We found a total of 12 compounds which fall in this category. Examples include: WS_2, RhF_3, $ZrCl_2$, and $GaInS_3$. The moduli **d**, **e** and **C** with other informations such as band gap, space group of these compounds are provided in the supplementary information.

We also observe that the piezoelectric compounds in the quasi-2D family of solids are clustered mainly in three specific space groups, *i.e.*, space group no. 36 ($Cmc2_1$), 160 ($R3m$), and 186 ($P6_3mc$). This is mainly a reflection of the population bias, as these are the three most frequently occurring non-centrosymmetric space groups in the quasi-2D family of crystals.

Table 1 shows that in 9 of the high-response quasi-2D piezoelectric compounds, the d_{15} component appears as d_{max}. Note that because of the freedom in choosing the in-plane axes, d_{15} and d_{24} are virtually indistinguishable (see the discussion section).

Table 1 List of top 20 candidate quasi-2D piezoelectric materials identified from the search, with their space group number (SG), calculated DFT band gap (E_g), maximal piezoelectric modulus (d_{max}), the d_{ij} component that appears as d_{max}, maximal e_{ij} (e_{max}), the component of **e** along the element of d_{ij} appearing as d_{max}.

Compound	SG	E_g(eV)	d_{max} (pC/N)	max d_{ij}	e_{max} (C/m^2)	max e_{ij}	$e_{d_{max}}$ (C/m^2)
In_2Te_5	9	0.7	351.7	d_{15}	2.6	e_{15}	2.6
PbS†	186	0.2	161.4	d_{33}	8.3	e_{33}	8.3
GeTe	160	0.6	148.4	d_{15}	3.3	e_{15}	3.3
$CuVO_3$	1	0.9	106.9	d_{22}	0.8	e_{32}	0.2
SnO	31	1.6	67.1	d_{22}	1.1	e_{22}	1.1
$BiInO_3$	33	2.8	56.1	d_{33}	4.7	e_{33}	4.7
Bi_2WO_6‡	41	1.7	54.1	d_{24}	3.9	e_{33}	2.9
NaI_3O_8	81	2.8	48.4	d_{14}	0.7	e_{31}	0.6
NaN_3	12	1.4	40.7	d_{36}	0.3	e_{34}	0.1
KSn_2F_5	143	3.0	40.5	d_{15}	0.3	e_{15}	0.3
MoV_2O_8	35	0.8	40.4	d_{33}	2.9	e_{33}	2.9
$TlBrO_3$	160	3.0	38.8	d_{24}	1.0	e_{24}	1.0
NaSnN	186	1.1	36.6	d_{15}	0.6	e_{15}	0.6
Cs_2Te_3‡	36	0.5	31.3	d_{36}	0.6	e_{11}	0.4
Bi_2MoO_6	61	1.7	28.7	d_{26}	1.6	e_{11}	1.3
AgI	186	1.3	27.8	d_{15}	0.3	e_{33}	0.1
SbF_2Cl_3	79	1.5	24.4	d_{15}	0.2	e_{33}	0.1
$MgCl_2$	115	4.9	23.5	d_{15}	0.2	e_{15}	0.2
$PbRb_2O_3$	36	1.3	22.2	d_{34}	0.7	e_{34}	0.7
$BiGeO_5$	9	2.3	21.1	d_{33}	3.0	e_{33}	3.0

† hypothetical structure
‡ dynamically-unstable structure

This journal is © The Royal Society of Chemistry [year]

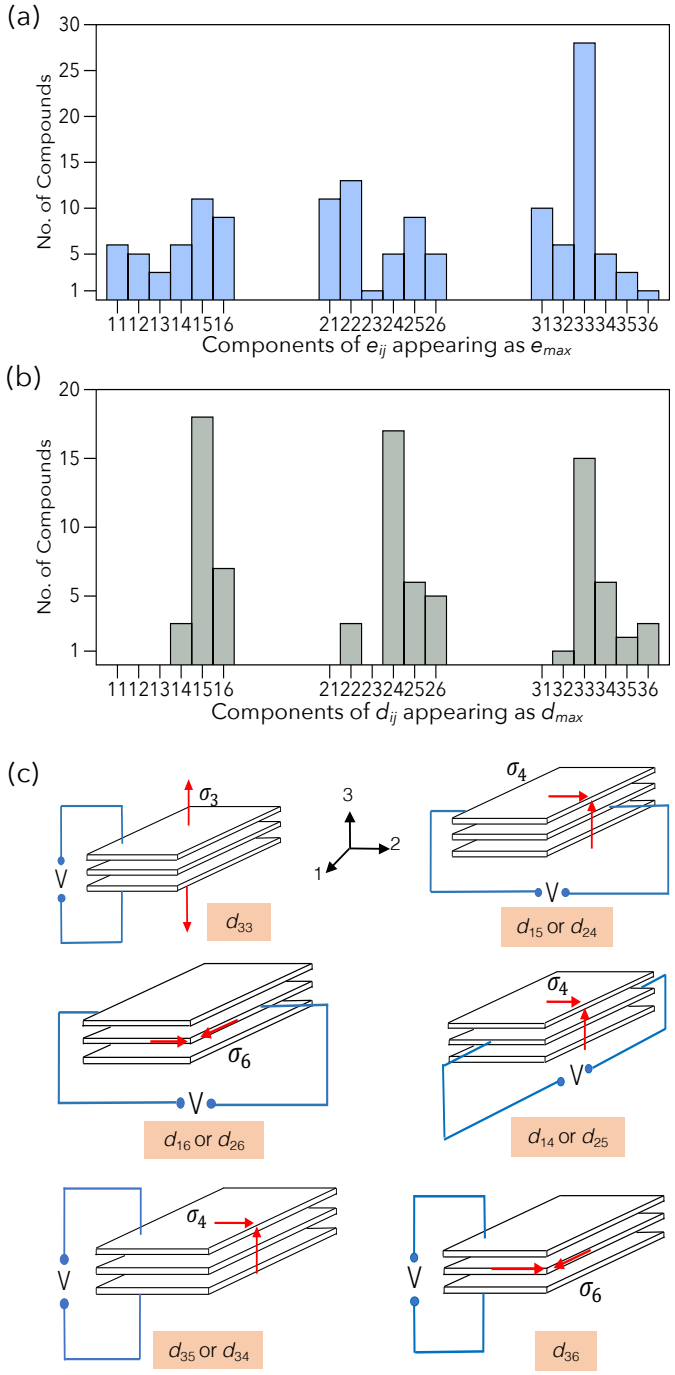

Fig. 6 Histogram of the maximum components of (a) the piezoelectric coefficient tensor, e_{max} and (b) piezoelectric modulus tensor, d_{max}. The most frequent e_{max} is e_{33}, whereas for d_{max} the most frequent maximum values are d_{15}, d_{24} and d_{33}. (c) Schematics of several important piezoelectric operating modes with their corresponding deformation types. The schematics of other relevant piezoelectric operating modes, *i.e.*, components of d_{ij} are provided in the supplementary information.

This component corresponds to the thickness shearing deformation where the material shears like a deck of cards in the in-plane direction, with no change in the other dimension. Materials with large d_{15} can be used in a variety of applications including: sensors, actuators, accelerometer, material testing structural health monitoring, non-destructive testing (NDT), and non-destructive evaluation (NDE).[66] The components of d_{ij} appearing as d_{max} usually coincide with the components of e_{ij} appearing as e_{max}. The distribution of different components of d_{ij} (and e_{ij}) appearing as d_{max} (and e_{max}) are discussed in more detail in the next section.

Another quantity that could influence the piezoelectric response is the band gap of the material. In this work, the band gaps are calculated at the DFT level and are also shown in Table 1 and supplementary information. Only about 1/3 of the studied materials are found to have DFT band gaps below 1 eV. Given the well known underestimation of band gaps in DFT based methods we do not think that materials with DFT band gaps larger than 1 eV would suffer from problems related to the existence of free charge carriers due to thermal fluctuations. However, for those with smaller gaps thermal fluctuation may cause sufficient number of free charge carriers, which may lower the polarization upon straining these materials despite having large piezoelectric moduli. Of course, provided that the real band gap is sufficiently close to the DFT one. For these materials, a more accurate assessment of the electronic structure might be needed before they are considered for applications.

In relation to the chemical composition and toxicity it is also important to note that currently, the most widely used piezoelectric material is lead zirconate titanate ($PbZr_{1-x}Ti_xO_3$ or PZT).[67] However, PZT causes significant environmental problems because of its high lead content.[67] Hence, significant efforts have been made to develop lead-free piezoelectric materials.[67–69] In our work, we have identified 44 candidates that do not contain any toxic elements including Pb. Out of 44 candidates, 33 of them have their piezoelectric modulus larger than AlN.

3.2 Role of van der Waals Interactions

In order to understand the role of van der Waals interactions on the piezoelectric response of quasi-2D materials, we analyze the relationships of e_{max} and d_{max} to the corresponding strain and stress components, respectively. A histogram showing the number of compounds with a given e_{ij} component appearing as e_{max} is shown in Figure 6 (a). We observe that the most frequent e_{max} is e_{33}. This indicates that in the majority of quasi-2D materials the largest piezoelectric response, as measured by the e_{ij}, is along the layer stacking direction. The reason for this behavior is that the relatively weak vdW interactions allow large charge redistribution in the layering direction upon straining the system.

On the other hand, the piezoelectric modulus tensor **d** relates stress to polarization and combines two types of effects: (1) amount of strain due to application of stress, and (2) amount of charge redistribution (polarization) due to resultant strain produced by the applied stress. A similar histogram of the d_{ij} components appearing as d_{max} is shown in Figure 6(b). We divide the d_{ij} components into three groups depending on the deformation types (stress components) and the polarization directions. The schematics of the polarization directions and the associated stress components are shown in Figure 6(c) together with the d_{ij} components connecting the two. Every component of d_{ij} represents a

separate piezoelectric operating mode. Schematics of all possible piezoelectric modes are provided in supplementary information.

Group I: Applied stress deforms van der Waals bonds and the measured polarization coincides with the direction of the deformations. The longitudinal mode (d_{33}) and shear modes (d_{15} and d_{24}) fall in this class. As evident from the histogram in Figure 6(b), these are the most frequently appearing d_{max} components. In our considered materials, the modes d_{24} and d_{15} are indistinguishable because of the arbitrariness of the choice of axes '1' and '2', while the axis '3' is fixed by layer stacking directions. In both of these modes, the same stress component (σ_4) is responsible for the deformation, which implies shearing of the van der Waals gaps. On the other hand, in the d_{33}, the applied stress axially deforms (stretches or compresses) van der Waals gaps. Hence, the large piezoelectric responses are achieved by deforming (axial or shear) the relatively soft van der Waals bonds. The bar-heights of d_{15} and d_{24} in the histogram of d_{max} in Figure 6(b) are larger compared to d_{33}. This is because the shearing resistance values (C_{44}) of quasi-2D materials are lower compared to their axial resistance values (C_{33}) (refer to Figure 3(b)).

Group II: Applied stress deforms van der Waals bonds, but the measuring polarization directions are different from their deformation directions. The face shear modes (d_{14} and d_{25}) and the thickness-extension modes (d_{31} and d_{32}) fall in this class. The schematics of d_{31} and d_{32} are provided in the supplementary information. Usually, the direction of polarization is facilitated by the direction of deformation. In such modes, the deformation directions are different from their measured polarization directions. This is the reason behind their low occurrence in the histogram of d_{max} though the van der Waals bond are deformed by the applied stress.

Group III: The van der Waals bond does not deform by the applied stress in these modes. This is why these modes do not appear frequently in the histogram of d_{max}. This includes length or width extension modes (d_{11} or d_{22}) and shearing modes of type d_{16} and d_{36}.

The above discussion implies that the large piezoelectric response is always accompanied and caused by the stress that deforms the "soft" van der Waals gaps either through stretching, compression, or shearing. In addition, the analysis of the maximal piezoelectric moduli and the associated stress components provide guidance to experimentalists of how thin films should be grown to utilize large d_{max}. It also describes what kind of mechanical actuation is necessary to achieve large piezoelectric response. This also helps in the design of new devices to take advantage of large d_{max}. Finally, these findings can open up a wide variety of devices based on their operation modes or based on new materials for non-conventional modes. For example, materials with large face-shear (d_{14}) mode response will be attractive for torsional applications, like novel gyroscopic sensors or high-precision torsional MEMS actuators.[66]

3.3 Axial Piezoelectric and Elastic Anisotropy

In addition to revealing new candidate piezoelectric materials and explaining the origin of strong piezoelectric response, we have also investigated the anisotropy in axial piezoelectric response in relation to the axial elastic anisotropy. We analyze how the response in the out-of-plane direction compares to the in-plane responses. The in-plane and out-of-plane directions in quasi-2D materials are trivial to define and are illustrated in Figure 1. We define the axial anisotropy in both elastic and piezoelectric responses by the ratio of the out-of-plane component to the in-plane component. Here, the in-plane component is defined by the arithmetic mean of the '11' and '22'-components (invariant to the choice of the in-plane axes), whereas the out-of-plane response is solely defined by the '33'-component. Hence, the axial anisotropy of **d**, **e**, and **C** can be expressed as $2d_{33}/(d_{11}+d_{22})$, $2e_{33}/(e_{11}+e_{22})$, and $2C_{33}/(C_{11}+C_{22})$ respectively. If the axial anisotropy equals or nearly equals 1 then the material is considered to be isotropic in the corresponding quantity responses with

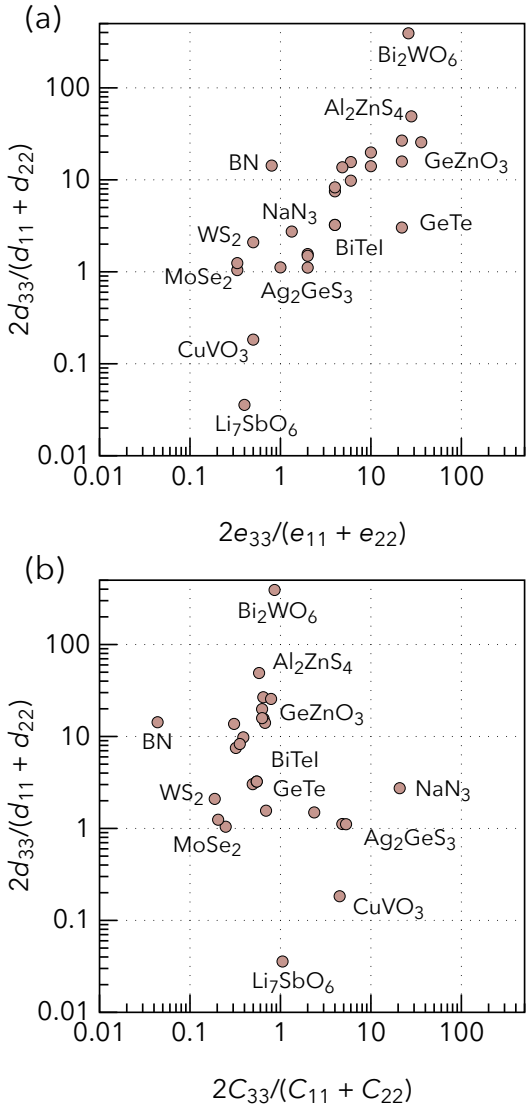

Fig. 7 Correlation between axial anisotropy, *i.e.*, out-of-plane to in-plane response ratio) of (a) **d** and **e** (b) **d** and **C**. The results reveal that majority of quasi-2D piezoelectric materials are dominated by out-of-plane piezoelectric responses (both in **e** and **d**) but elastically they are dominated in in-plane direction.

This journal is © The Royal Society of Chemistry [year]

respect to the in-plane and out-of-plane directions. If the axial anisotropy is greater (or lower) than 1 the response of the material is dominated in out-of-plane (in-plane) direction. By dominant, we mean the value of the property is larger in that specific crystallographic direction *i.e.* in-plane or out-of-plane.

All possible correlations among the axial anisotropy of **d**, **e**, and **C** have been investigated. The correlation between axial anisotropy of **d** with respect to the axial anisotropy of **e** and **C** are shown in Figure 7 (a) and (b) respectively. From the comparative studies between Figure 7 (a) and (b), we see that the axial anisotropy of **d** is mainly dictated by the axial anisotropy of **e** not by the axial anisotropy of **C**. The plot between axial anisotropy of **C** and **e** is provided in the supplementary information.

From Figure 7a and 7b, we observe that most layered materials have axial piezoelectric anisotropy (both in **d** and **e**) > 1 and axial elastic anisotropy < 1. This indicates that majority of these quasi-2D compounds have large C_{11} and C_{22} compared to C_{33}, whereas in cases of d and e, they have large e_{33} and d_{33} compared to e_{11} or e_{22} and d_{11} or d_{22}. This result corroborates the correlation between elastic softness and large piezoelectric response, *i.e.*, the large piezoelectric responses are observed in elastically softer directions. We found quasi-2D piezoelectric compounds such as $CuVO_3$ and Li_7SbO_6 are dominated by in-plane piezoelectric response. Compounds such as Bi_2WO_6, Li_7SbO_6, and $GeZnO_3$ are nearly isotropic in their axial elastic responses but highly anisotropic in axial piezoelectric responses (see supplementary information for detail explanation).

4 Conclusions

In conclusion, we performed a large-scale computational (first-principles) assessment of the bulk piezoelectric properties of layered (quasi-2D) vdW bonded materials. In our study, we concentrate on the piezoelectric modulus as the measure of the piezoelectric response, which relates mechanical stress and electric polarization and depends on a combination of charge redistribution due to strain and the amount of strain produced by the stress. Overall, out of 135 non-centrosymmetric quasi-2D binary and ternary structures from ICSD we have discovered 51 materials with piezoelectric response larger than that of AlN, a well-known piezoelectric materials used in applications. Out of these 51 systems, we find three with the piezoelectric modulus even larger than that of $PbTiO_3$ that has the piezoelectric modulus among the largest known. More importantly, 33 out of the 51 layered compounds do not contain any toxic elements including Pb. Our results also reveal that the large piezoelectric modulus in vdW systems is directly enabled by the vdW interactions between layers as in majority of compounds the large components of the piezoelectric modulus tensor couple to the stress components that imply deformations (both shear and axial) of the "soft" vdW bonds between layers. Our results suggest that quasi-2D layered materials are a rich structural space for discovering new piezoelectric materials.

Conflicts of interest

There are no conflicts of interest to declare.

Acknowledgements

The authors gratefully acknowledge the support of the National Science Foundation through Grant No. DMREF-1534503. The calculations were performed using the high-performance computing facilities at National Renewable Energy Laboratory (NREL) and at Colorado School of Mines (the Golden Energy Computing Organization) .

References

1 B. Jaffe, *Piezoelectric Ceramics*, Elsevier Science, 2012.
2 K. Uchino, *Piezoelectric Actuators and Ultrasonic Motors*, Springer US, 1996.
3 S. Liu, L. Wang, Z. Wang, Y. Cai, X. Feng, Y. Qin and Z. L. Wang, *ACS Nano*, 2018, **12**, 1732–1738.
4 R. Weigel, D. P. Morgan, J. M. Owens, A. Ballato, K. M. Lakin, K. Hashimoto and C. C. W. Ruppel, *IEEE Transactions on Microwave Theory and Techniques*, 2002, **50**, 738–749.
5 W. Wu and Z. L. Wang, *Nature Reviews Materials*, 2016, **1**, 16031.
6 K. Uchino, *Smart Materials and Structures*, 1998, **7**, 273.
7 Y. Saito, H. Takao, T. Tani, T. Nonoyama, K. Takatori, T. Homma, T. Nagaya and M. Nakamura, *Nature*, 2004, **432**, 84.
8 R. Armiento, B. Kozinsky, G. Hautier, M. Fornari and G. Ceder, *Physical Review B*, 2014, **89**, 134103.
9 R. Armiento, B. Kozinsky, M. Fornari and G. Ceder, *Physical Review B*, 2011, **84**, 014103.
10 M. De Jong, W. Chen, H. Geerlings, M. Asta and K. A. Persson, *Scientific Data*, 2015, **2**, year.
11 L. Dong, J. Lou and V. B. Shenoy, *ACS Nano*, 2017, **11**, 8242–8248.
12 M. N. Blonsky, H. L. Zhuang, A. K. Singh and R. G. Hennig, *ACS Nano*, 2015, **9**, 9885–9891.
13 W. Li and J. Li, *Nano Research*, 2015, **8**, 3796–3802.
14 H. Yin, J. Gao, G. P. Zheng, Y. Wang and Y. Ma, *The Journal of Physical Chemistry C*, 2017, **121**, 25576–25584.
15 K.-A. N. Duerloo, M. T. Ong and E. J. Reed, *The Journal of Physical Chemistry Letters*, 2012, **3**, 2871–2876.
16 R. Hinchet, U. Khan, C. Falconi and S.-W. Kim, *Materials Today*, 2018.
17 M. M. AlyoÌĹruÌĹk, Y. Aierken, D. CÌğakır, F. M. Peeters and C. Sevik, *The Journal of Physical Chemistry C*, 2015, **119**, 23231–23237.
18 M. T. Ong and E. J. Reed, *ACS nano*, 2012, **6**, 1387–1394.
19 M. T. Ong, K.-A. N. Duerloo and E. J. Reed, *The Journal of Physical Chemistry C*, 2013, **117**, 3615–3620.
20 S. Chandratre and P. Sharma, *Applied Physics Letters*, 2012, **100**, 023114.
21 J. F. Nye, *Physical properties of crystals: their representation by tensors and matrices*, Oxford University Press, 1985.
22 *We refer **e**, which couple strain and electric displacement as piezoelectric coefficient tensor or piezoelectric stress coefficients. **d**, which couple stress with electric displacement, are referred as*

piezoelectric modulus tensor or piezoelectric strain modulus. In both cases, we express the individual matrix elements in standard reduced Voigt notation.

23 W. Voigt, *Lehrbuch der kristallphysik (mit ausschluss der kristalloptik)*, Springer-Verlag, 2014.

24 R. Lec and W. Soluch, Ultrasonics Symposium, 1977, 1977, pp. 389–392.

25 A. Pramanick, D. Damjanovic, J. E. Daniels, J. C. Nino and J. L. Jones, *Journal of the American Ceramic Society*, 2011, **94**, 293–309.

26 Z. Li, M. Grimsditch, X. Xu and S. K. Chan, *Ferroelectrics*, 1993, **141**, 313–325.

27 K. Lefki and G. Dormans, *Journal of Applied Physics*, 1994, **76**, 1764–1767.

28 A. V. Sotnikov, H. Schmidt, M. Weihnacht, E. P. Smirnova, T. Y. Chemekova and Y. N. Makarov, *IEEE transactions on ultrasonics, ferroelectrics, and frequency control*, 2010, **57**, year.

29 Z.-G. Ye, *Handbook of advanced dielectric, piezoelectric and ferroelectric materials: Synthesis, properties and applications*, Elsevier, 2008.

30 G. Bergerhoff, R. Hundt, R. Sievers and I. Brown, *Journal of Chemical Information and Computer Sciences*, 1983, **23**, 66–69.

31 A. Belsky, M. Hellenbrandt, V. L. Karen and P. Luksch, *Acta Crystallographica Section B: Structural Science*, 2002, **58**, 364–369.

32 P. Gorai, E. S. Toberer and V. Stevanović, *Journal of Materials Chemistry A*, 2016, **4**, 11110–11116.

33 M. Ashton, J. Paul, S. B. Sinnott and R. G. Hennig, *Physical Review Letter*, 2017, **118**, 106101.

34 N. Mounet, M. Gibertini, P. Schwaller, D. Campi, A. Merkys, A. Marrazzo, T. Sohier, I. E. Castelli, A. Cepellotti, G. Pizzi and N. Marzari, *Nature Nanotechnology*, 2018, 1.

35 G. Cheon, K.-A. N. Duerloo, A. D. Sendek, C. Porter, Y. Chen and E. J. Reed, *Nano Letters*, 2017, **17**, 1915–1923.

36 S. Lebègue, T. Björkman, M. Klintenberg, R. M. Nieminen and O. Eriksson, *Physical Review X*, 2013, **3**, 031002.

37 G. Kresse and J. Hafner, *Physical Review B*, 1993, **47**, 558.

38 G. Kresse and J. Furthmüller, *Physical Review B*, 1996, **54**, 11169.

39 J. c. v. Klimeš, D. R. Bowler and A. Michaelides, *Physical Review B*, 2011, **83**, 195131.

40 J. Klimeš, D. R. Bowler and A. Michaelides, *Journal of Physics: Condensed Matter*, 2009, **22**, 022201.

41 S. Baroni, S. De Gironcoli, A. Dal Corso and P. Giannozzi, *Reviews of Modern Physics*, 2001, **73**, 515.

42 S. Baroni, P. Giannozzi and A. Testa, *Physical Review Letter*, 1987, **58**, 1861.

43 X. Gonze, *Physical Review A*, 1995, **52**, 1096.

44 Y. Le Page and P. Saxe, *Physical Review B*, 2002, **65**, 104104.

45 B. Narayanan, I. E. Reimanis, E. R. Fuller Jr and C. V. Ciobanu, *Physical Review B*, 2010, **81**, 104106.

46 S. Manna, G. L. Brennecka, V. Stevanović and C. V. Ciobanu, *Journal of Applied Physics*, 2017, **122**, 105101.

47 S. Manna, K. R. Talley, P. Gorai, J. Mangum, A. Zakutayev, G. L. Brennecka, V. Stevanović and C. V. Ciobanu, *Physical Review Applied*, 2018, **9**, 034026.

48 J. P. Perdew, K. Burke and M. Ernzerhof, *Physical Review Letter*, 1996, **77**, 3865.

49 A. Jain, S. P. Ong, G. Hautier, W. Chen, W. D. Richards, S. Dacek, S. Cholia, D. Gunter, D. Skinner, G. Ceder and K. A. Persson, *APL Materials*, 2013, **1**, 011002.

50 B. Khanbabaee, E. Mehner, C. Richter, J. Hanzig, M. Zschornak, U. Pietsch, H. Stöcker, T. Leisegang, D. Meyer and S. Gorfman, *arXiv preprint arXiv:1605.07490*, 2016.

51 N. Marom, A. Tkatchenko, M. Scheffler and L. Kronik, *Journal of Chemical Theory and Computation*, 2009, **6**, 81–90.

52 M. Born, Mathematical Proceedings of the Cambridge Philosophical Society, 1940, pp. 160–172.

53 F. Mouhat and F.-X. Coudert, *Physical Review B*, 2014, **90**, 224104.

54 P. Gorai, E. S. Toberer and V. Stevanović, *Physical Chemistry Chemical Physics*, 2016, **18**, 31777–31786.

55 *A Python framework for high-throughput first-principles calculations*, https://github.com/pylada.

56 J. Y. Li, *Journal of the Mechanics and Physics of Solids*, 2000, **48**, 529–552.

57 S. Grimme, J. Antony, S. Ehrlich and H. Krieg, *The Journal of chemical physics*, 2010, **132**, 154104.

58 A. Tkatchenko and M. Scheffler, *Physical review letters*, 2009, **102**, 073005.

59 D. Zagorac, K. Doll, J. C. Schön and M. Jansen, *Physical Review B*, 2011, **84**, 045206.

60 T. Chattopadhyay, J. X. Boucherle and H. G. vonSchnering, *Journal of Physics C: Solid State Physics*, 1987, **20**, 1431.

61 H. Sutherland, J. Hogg and P. Walton, *Acta Crystallographica Section B: Structural Crystallography and Crystal Chemistry*, 1976, **32**, 2539–2541.

62 M.-A. Dubois and P. Muralt, *Applied Physics Letters*, 1999, **74**, 3032–3034.

63 K. Chuntonov, A. Orlov, S. Yatsenko, Y. N. Grin and L. Miroshnikova, *Izv. Akad. Nauk SSSR, Neorg. Mater*, 1982, **18**, 1113–1116.

64 R. Wolfe, R. Newnahm and M. Kay, *Solid State Communications*, 1969, **7**, 1797–1801.

65 V. E. Bottom, *Journal of Applied physics*, 1970, **41**, 3941–3944.

66 G. Boivin, P. Bélanger and R. J. Zednik, THERMEC 2016, 2017, pp. 637–641.

67 T. R. Shrout and S. J. Zhang, *Journal of Electroceramics*, 2007, **19**, 113–126.

68 T. Takenaka and H. Nagata, *Journal of the European Ceramic Society*, 2005, **25**, 2693–2700.

69 P. Baettig, C. F. Schelle, R. LeSar, U. V. Waghmare and N. A. Spaldin, *Chemistry of materials*, 2005, **17**, 1376–1380.

This journal is © The Royal Society of Chemistry [year]